Taylor & Francis
Taylor & Francis Group

Journal of Experimental Nanoscience

ISSN: 1745-8080 (Print) 1745-8099 (Online) Journal homepage: informahealthcare.com/journals/tjen20

Enhanced transdermal delivery of carvedilol using nanoemulsion as a vehicle

Mohammad Rizwan, Mohammed Aqil, Adnan Azeem, Sushama Talegaonkar, Yasmin Sultana & Asgar Ali

To cite this article: Mohammad Rizwan, Mohammed Aqil, Adnan Azeem, Sushama Talegaonkar, Yasmin Sultana & Asgar Ali (2010) Enhanced transdermal delivery of carvedilol using nanoemulsion as a vehicle, Journal of Experimental Nanoscience, 5:5, 390-411, DOI: 10.1080/17458080903583964

To link to this article: https://doi.org/10.1080/17458080903583964

Published online: 05 Nov 2010.

Journal of Experimental Nanoscience
Vol. 5, No. 5, October 2010, 390–411

Taylor & Francis
Taylor & Francis Group

Enhanced transdermal delivery of carvedilol using nanoemulsion as a vehicle

Mohammad Rizwan, Mohammed Aqil*, Adnan Azeem, Sushama Talegaonkar, Yasmin Sultana and Asgar Ali

Department of Pharmaceutics, Faculty of Pharmacy, Hamdard University, New Delhi 110062, India

(*Received 8 October 2009; final version received 28 December 2009*)

The aim of the present study was to develop nanoemulsion as a possible vehicle for enhanced transdermal penetration of carvedilol (CVD). For screening of nanoemulsion components, solubility of CVD in oils, surfactants and co-surfactants was determined. Various surfactants and co-surfactants were screened for their ability to nanoemulsify the selected oily phases. The obtained results indicated that Acconon CC6® had shown good nanoemulsification efficiency (minimum surfactant required $S_{min} = 46.52\%$ w/w) among the selected surfactants and further improved in presence of CO-20® ($S_{min} = 37.11\%$ w/w). The ranges of nanoemulsion existence were delineated through the construction of the pseudo-ternary phase diagram at different ratio of surfactant mixture (*S*/Co*S*), and various nanoemulsions were selected from phase diagram of *S*/Co*S* ratio 1 : 1. The effect of content of oil and *S*/Co*S* (1 : 1) on the skin permeation of CVD was evaluated through an excised wistar rat skin using Franz diffusion cell. All the nanoemulsions showed a high skin permeation rate (92.251–161.53 μg/cm^2/h), good enhancement ratio (3.5–6.2) and high permeability coefficient in comparison to control groups. The optimised nanoemulsion formulation with the highest skin permeation rate (161.53 μg/cm^2/h) consisted of 0.25% w/w CVD, 12.5% w/w Miglyol 810®, 50% w/w Acconon CC6®/CO-20® (1 : 1) and water. The above formulation had the smallest mean globules size (9.28 nm). The superior transdermal flux of CVD may be due to nanorange size of oil globules that lead to intimate contact with the skin layer. These studies suggest that the nanoemulsion system is a promising vehicle for the transdermal delivery of CVD.

Keywords: nanoemulsion; carvedilol; transdermal delivery; pseudo-ternary phase diagram

1. Introduction

Carvedilol (CVD), a racemic mixture of two enantiomers, has β-adrenoceptor blocking activity and α1-receptor blocking activity. It is extensively used in the long-term management of hypertension and angina pectoris, and as an adjunct to standard therapy in symptomatic heart failure [1]. It is well absorbed from the gastrointestinal tract, but it is subjected to considerable first-pass metabolism in the liver which leads to low absolute

*Corresponding author. Email: aqilmalik@yahoo.com

ISSN 1745–8080 print/ISSN 1745–8099 online

DOI: 10.1080/17458080903583964
http://www.informaworld.com

oral bioavailability (25–30%) [2]. The drug is well tolerated and has relatively few adverse effects. It is highly lipophilic and extremely protein bound. It is practically insoluble in water, gastric fluid and intestinal fluid [3]. Due to low bioavailability, frequent dosing for a long period is required, in addition, CVD insolubility in water and gastrointestinal fluid causes many disadvantages associated with oral administration [4,5]. Therefore, an alternate route of administration is required for sustained therapeutic action to surmount the disadvantages of oral administration and also for improving the compliance of patients.

The skin provides a favourable route of drug administration to the formulator with a surface area of about $2\,m^2$ in an adult human [6]. Transdermal drug delivery offers many advantages over other traditional routes of drug delivery, such as avoidance of hepatic metabolism, controlled release of drug, steady blood-level profile, leading to reduced systemic side effects and, sometimes improved efficacy over other dosage forms, user friendly, painless and offers multi-day dosing and thus, consequently, improves the compliance of patients. Despite many advantages, the impervious barrier nature of the skin makes it difficult for most drugs to be delivered into and through it. Consequently, to penetrate the strong skin barrier, especially stratum corneum (SC), many strategies have been employed. These techniques include the use of chemical penetration enhancers [7], iontophoresis [8], electroporation or sonophoresis [9] or encapsulating the drug in vesicular delivery systems [10,11].

Recently, micro/nanoemulsion (NE) as a vehicle for dermal/transdermal delivery has garnered a lot of attention for enhanced skin penetration of both lipophilic and hydrophilic drugs [12–19]. NE is a clear, transparent/translucent, optically isotropic system of oil, water, surfactant and co-surfactant at appropriate ratios. It is an ideal liquid vehicle for drug delivery due to its high solubilisation capacity, thermodynamic stability (long shelf life), ease of formulation, low viscosity and small droplet size (<150 nm) [20,21]. Application of NE as a vehicle for transdermal delivery system has many additional advantages, like high thermodynamic activity of drug towards skin due to high solubilsation favours its skin partitioning and small droplets have better chance to adhere to SC and to transport drugs in a more controlled manner [18,20]. The ingredients of NE may act as permeation enhancers, and the hydration effect of the formulation further reduces the diffusion barrier of SC and increases the permeation rate of drug via skin [20,22–24].

CVD has been delivered transdermally using matrix type patch [25,26], NE formulation [27]. In addition, different penetration enhancers were studied for enhanced skin permeation [28–31]. Dixit et al. (2008) reported transdermal delivery of CVD using NE vehicle consisted of oleic acid: isopropyl myristate (as oil), Tween 80/Transcutol P (as surfactant/co-surfactant) and distilled water [27]. Oleic acid is a long-chain fatty acid, which showed interaction with CVD, was observed during this study and was also reported by Wei and co-workers [32]. In addition, oleic acid is not easy to nanoemulsify in comparison to medium-chain triglyceride (MCT) [33]. Thus, the aim of this study was to select a suitable oil that could solubilise the drug as well as that can be easily nanoemulsify by selected non-ionic surfactants. Minimum surfactants (S_{min}) required to nanoemulsify the various oils were determined. Non-ionic surfactants were selected to minimise skin irritation and charge disruption of the system for the formulation development. NE was developed after screening of oils and surfactants that could solubilise sufficiently high

amount of the drug; non-ionic surfactants were selected on the basis of their nanoemulsifying ability of oils. Furthermore, Pseudo-ternary phase diagrams were constructed to delineate the NE existence region and their concentration ranges using selected components. Effect of oil and surfactant concentration on skin permeation of the drug was also studied. Hence, the major objective of this study is to develop a stable NE formulation for enhanced skin penetration having sustained therapeutic action.

2. Materials and methods

2.1. *Materials*

CVD (purity 99%) was a kind gift from Wockhardt Research Center, Aurangabad (Maharashtra, India). Plurol Oleique® (polyglyceryl-6-dioleate), Capryol 90® (propylene glycol monocaprate), Labrasol® (polyoxyethylene 8 caprylic/capric glycerides), Plurol Isostearique® (polyglyceryl-6-isostearate), Lauroglycol 90® (propylene glycol monolaurate), Labrafil M®1944CS and Labrafil M® 2125CS (oleyl and linoleyl polyoxylglycerides, respectively) and Transcutol P (diethylene glycol monoethyl ether) were gift samples from Colorcon Asia Pvt Ltd (Mumbai, India). Capmul PG-8® (propylene glycol monocaprylate) and Acconon CC6® (polyoxyethylene 6 caprylic/capric glycerides) were gifts from Abitec Corporation (Janesville, WI), Isopropyl myristate (IPM), Isopropyl palmitate (IPP), oleic acid, Tween 80, Tween 20, Span 20 and ethanol were purchased from E-Merck (Mumbai, India). Cremophore RH40® (polyoxyl 40 hydrogenated castor oil), PEG-200, PEG-400, and propylene glycol were purchased from Sigma Aldrich (St. Louis, MO). Olive oil and CO-20 (PEG-20 castor oil) were free samples from Nikko Chemicals (Japan). Miglyol 810® (caprylic/capric triglyceride) was purchased from Sasol Germany GmbH (Witten, Germany). All other chemicals and reagents used in the study were of AR grade. Purified water was obtained from Milli-Q purification system (Milford, USA).

2.2. *Solubility studies*

The solubility of CVD in oils, surfactant, co-surfactants and solvents were determined by the shake flask method. Briefly, an excess amount of CVD was added to each cap vial containing 2 ml of the selected vehicles. After sealing, the mixtures were vortexed in order to facilitate proper mixing of CVD with vehicles. Mixtures were then shaken for 72 h in a water bath shaker (Remi, Mumbai, India) maintained at room temperature. It was centrifuged at 4000 rpm for 15 min and supernatants were filtered through membrane filter (0.45 μm, Pall Lifesciences, Mumbai, India). Filtrate was suitably diluted with methanol and quantified by in-house developed HPLC method.

2.3. *Screening of surfactants for emulsifying ability*

Nanoemulsifying ability (S_{min}) of various surfactants, such as Labrasol®, Acconon CC6® and Tween 80 was screened for different oils. Oils employed were olive oil, oleic acid, Labrafil M1944CS®, Labrafil M2125CS®, Capmul PG8® and Miglyol 810®. The amount of surfactants (S_{min}) required to completely solubilise equal mixture of oil and water (1 : 1) to form a single-phase NE was determined at room temperature. The mixture was titrated

with selected surfactant untill the mixture turned from turbid to clear isotropic mixture. The amount of surfactants added to mixtures that change the appearance of mixture from turbid to clear transparent on visual observation was termed as S_{min}. The NEs were allowed to stand for 24 h and their transmittance was assessed at 650 nm by UV-1601, a double-beam spectrophotometer (Shimadzu, Japan), using milli-q water as blank [34]. Based on solubility data and S_{min} values obtained, Miglyol 810® and Acconon CC6® were selected as oil and surfactant, respectively, for further studies.

2.4. *Screening of co-surfactants*

Studies were performed to assess relative efficacy of co-surfactants for nanoemulsification of Miglyol 810® (as oil) with Acconon CC6® (as surfactant) and to select the best co-surfactant from a large pool of co-surfactants available. The co-surfactants selected for study were polyglycerol esters (Plurol Oleique®), ethoxylated non-ionic surfactants (Cremophore RH40®, CO-20® and Labrasol®), Transcutol P® and ethanol. The mixtures of surfactant and co-surfactants (*S*/Co*S*) in a ratio of 1 : 1 were prepared. In order to find $SCoS_{min}$ (minimum surfactant/co-surfactant mixture required for nanoemulsification), oil and water (the water/oil ratio 1 : 1 was kept constant) mixture was titrated with each *S*/Co*S* mixture under continuous mixing at Vibrax mixer. After each addition, the samples were observed visually for clarity, the clear and transparent mixture was called as NE. The NEs were allowed to stand for 24 h and their transmittance was measured at 650 nm by UV-1601 double-beam spectrophotometer using milli-q water as blank.

In addition, NE existence region at a fixed *S*/Co*S* ratio of 1 : 1 was taken as another parameter for co-surfactant selection (method presented in Section 2.5). The *S*/Co*S* mixture that showed a high nanoemuslification efficiency (least S/CoS_{min} value), and maximised existence area of NE in pseudo-ternary phase diagram was taken as the best surfactant/co-surfactant mixture for selected oil nanoemulsification.

2.5. *Construction of pseudo-ternary phase diagrams*

Pseudo-ternary phase diagrams of oil, surfactant/co-surfactant and water were constructed in order to obtain the concentration range of each component for the existing region of NEs. For each pseudo-ternary phase diagram at a specific *S*/Co*S* ratio, the mixtures containing oil, surfactant and co-surfactant were prepared with the weight ratio of oil to mixture of surfactant and co-surfactant at 10 : 90, 20 : 80, 30 : 70, 40 : 60, 50 : 50, 60 : 40, 70 : 30, 80 : 20, 90 : 10, 20 : 100, 20 : 140 and 20 : 160, respectively. Purified milli-q water was added drop by drop to each weight ratio of oil and *S*/Co*S* and mixed by vortexing. Different combinations of oil and *S*/Co*S* were studied to define the boundaries of NE region precisely formed in the phase diagrams study. NE was selected by visual observation, which is clear, transparent and easily flowable mixture of oil, *S*/Co*S* and water. The method employed for selection of co-surfactant from various co-surfactants at fixed SCoS ratio (1 : 1), whereas, different ratios (*S*/Co*S* ratios i.e. 1 : 0, 1 : 1, 2 : 1, 4 : 1 and 1 : 2) of Acconon CC6® and CO-20® were tried to optimise the *S*/Co*S* ratio that showed maximal NE existence region.

Pseudo-three-component phase diagram was drawn with one axis representing aqueous phase, the other representing oil and the third representing a mixture of surfactant and

co-surfactant at fixed weight ratios (*S*/Co*S* ratio). Based on these diagrams, appropriate concentration of each component was selected for the preparation of NE containing CVD.

2.6. *Selection of nanoemulsion formulations*

The NE formulations were selected from constructed pseudo-ternary phase diagrams of *S*/Co*S* ratio 1 : 1, which showed the largest NE existence region. Out of several NEs, those NEs were selected in which the percentage of oil was sufficient to dissolve the desired dose of CVD. Furthermore, NEs were prepared by varying the oil and surfactant mixture concentration to investigate the effect of oil and surfactant mixture on the skin permeation rate. The content of oil and *S*/Co*S* mixture was varied from 10–20% w/w and 35–50% w/w, respectively, in NEs. The selected NEs were subjected to thermodynamic stability studies and physical characterisation.

2.7. *Characterisation of nanoemulsion*

2.7.1. *Thermodynamic stability studies*

The objective of thermodynamic stability is to evaluate the phase separation, effect of temperature variation on NEs and to avoid the metastable formulations.

Centrifugation test: NEs selected were subjected to centrifugation at 15,000 rpm for 15 min. The NEs that did not show any phase separation were taken for the freeze thaw stress test.

Freeze thaw cycle: The NEs were submitted for three freeze thaw cycles between −20°C and +25°C with storage at each temperature for not less than 48 h and assessed for any phase separation.

2.7.2. *Analysis of droplet size and distribution*

The average droplet size and size distribution of the NEs were determined by the photon correlation spectroscopy on a Zetasizer 1000 HS (Malvern Instruments, Worcestershire, UK). The measurement was carried out at a fixed angle of 90°C at 25°C with the samples diluted approximately 100 times with milli-q water. The droplet size of the NEs was described by the cumulants mean (*z*-average) diameter and the size distribution was described by the polydispersity index (PI).

2.7.3. *Transmission electron microscopic analysis*

The morphology and structure of NE was observed using Morgagni 268-D transmission electron microscope (Fei 155 Company, The Netherlands) operating at 70 kV capable of 156 point-to-point resolution. NE formulations were diluted with water (1 : 100). One drop of diluted samples was applied on a carbon-coated grid, stained with one drop of 3% phosphotungstic acid (PTA) and allowed to dry for 10 min before observation under the electron microscope.

2.7.4. *Viscosity measurement*

The viscosities of various NEs were measured without dilution using Brookfield DV III ultra V6.0 RV cone and plate rheometer (Brookfield Engineering Laboratories, Inc., Middleboro, MA, USA) using spindle #CPE-40 set at 50 rpm at 25 ± 0.5°C.

2.7.5. *Refractive index and pH measurement*

The refractive index of the NEs was measured using an Abbe refractometer (Bausch and Lomb Optical Company, Rochester, NY, USA) by placing one drop of sample on the slide. pH of NE was determined by digital pH meter (Mettler Toledo MP 220, Greifensee, Switzerland) at $25 \pm 1^{\circ}C$.

2.7.6. *Transmittance studies*

The per cent transmittance of the prepared NEs was measured at 650 nm using UV-1601 double-beam spectrophotometer keeping milli-q water as blank.

2.8. Ex vivo *skin permeation studies*

The abdominal skin samples were obtained from Wistar rats weighing 200 ± 10 g. The *ex vivo* permeation studies were performed using an automated transdermal diffusion cell sampling system (SFDC 6, LOGAN Instruments, NJ, USA). The system consisted of three side-by-side and three vertical diffusion cells with an effective diffusion area of $0.636\,cm^2$. The skin was placed between donor and receiver compartments of vertical diffusion cells with SC side up. The receiver compartments were filled with 5 ml of freshly prepared 5% v/v Transcutol P® in isotonic phosphate buffer (pH 7.4) vehicle to ensure sink condition and stirred at 600 rpm throughout the experiment. The temperature of receiver compartments was maintained at $37 \pm 0.2^{\circ}C$ with recirculating pre-heated water. One gram of test NE formulation containing 2.5 mg of CVD was placed in donor compartment and covered with parafilm (3M, Chicago, IL, USA). For each experiment, 500 µl of samples were withdrawn from the receptor compartment at different time intervals and immediately replenished with the same amount of fresh vehicle. All the samples were filtered through 0.45 µm membrane filter and analysed by HPLC.

2.9. *Data analysis*

The cumulative amount of drug permeated was plotted as a function of time. Skin permeation rate (flux, *Jss*) of drug at a steady state was calculated from the slope of linear portion of the cumulative amount permeated through the rat skin per unit area versus time plot. The intercept on the *x*-axis was taken as the lag time (T_{lag}, h). The permeability coefficient of Pb was calculated by dividing flux by drug load in formulation, and enhancement ratio (ER) was calculated on dividing the flux of formulations by the flux from control vehicle.

2.10. *Statistical analyses*

All the experimental values are reported as mean ± SD from three independent experiments. Data were statistically analysed by one-way ANOVA for more than two groups, and student's *t*-test was applied for comparison of two groups. The evaluations were made using the GraphPad Prism® version 5 software and results considered statistically significant at 95% confidence interval (i.e. $p < 0.05$).

3. Results and discussion

3.1. *Solubility studies*

Appropriate selection of oil and surfactant is the most important part for development of NE. The oil and surfactant that has greater solubilising capacity are best suited for the development of NE, because high solubility of a drug in the oil phase is important for the NE to maintain the drug in solubilised form and also for drug permeation through the skin [23]. Consequently, to screen appropriate components for the preparation of NE, the solubility of CVD in various oils and non-ionic surfactants were performed and the results are shown in Table 1. Oleic acid showed the highest solubility of CVD of 105.29 ± 13.72 mg/ml, which is the best among all investigated oils. Other oils that showed significantly high solubility as compared to water and other oils are Miglyol 810® (31.46 ± 4.27 mg/ml) and Capmul PG8 (27.47 ± 5.13 mg/ml; $p < 0.05$; Table 1). On the basis of high solubilisation potential, oleic acid could be a suitable oil phase for development of NE.

But, choice of the oil phase is sometimes difficult and quite challenging because it is important for the area of existence of NE in phase diagram, and to ensure maximum solubilisation of drug in the resultant dispersion as well as stability of drug in it [21,35]. Thus, further scrutiny of oils was performed on the basis of solubilising capacity by selected surfactants. The amount of surfactant required to completely homogenise equal masses of oil and water to form a single phase NE (S_{min}) was determined for different oils.

Skin irritation is the major problem with many anionic and cationic surfactants; also high concentration of surfactants could aggravate the irritation. Non-ionic surfactants are less toxic than ionic surfactants and have lower critical micelle concentration (CMCs) than their ionic counterparts. Therefore, considering the safety-related issue, various non-ionic surfactants/co-surfactants were selected for solubility and nanoemulsification efficiency studies. Transcutol P® had high and fast solubilising capacity for CVD (184.02 ± 21.03 mg/ml). Labrasol® (53.05 ± 7.84 mg/ml)

Table 1. Solubility of carvedilol in various vehicles (oils, surfactants and water).

Oil	Solubility (mg/ml)	Surfactants	Solubility (mg/ml)	Surfactants/ vehicle	Solubility (mg/ml)
Oleic acid	105.29 ± 13.72	Acconon CC6®	44.32 ± 6.89	Transcutol P®	184.02 ± 21.03
Capmul PG8®	27.47 ± 5.13	Labrasol®	53.05 ± 7.84	Plurol isostearique®	8.56 ± 1.10
Miglyol 810®	31.46 ± 4.27	Tween 80	21.50 ± 2.06	PEG-200	31.38 ± 9.49
Labrafil M 2125®	21.17 ± 1.06	Cremophore RH40®	11.06 ± 1.38	PEG-400	43.33 ± 3.15
Olive oil	7.20 ± 0.43	Tween 20	17.72 ± 6.14	Propylene glycol	7.31 ± 0.86
IPP	4.89 ± 0.56	Span 20	3.1 ± 0.31	Ethanol	10.74 ± 0.99
IPM	3.72 ± 0.12	CO-20®	22.78 ± 2.15	Water	Not detectable
Labrafil M 1944®	22.36 ± 2.13	Lauroglycol 90®	9.42 ± 0.94		

Note: mean $\pm$ SD; $n = 3$.

showed a good solubility followed by Acconon CC6 (44.32 ± 6.89 mg/ml), PEG-400 (43.33 ± 3.15 mg/ml), PEG-200 (31.38 ± 9.49 mg/ml), CO-20 (22.78 ± 2.15 mg/ml) and Tween 80 (21.50 ± 2.06 mg/ml) (Table 1). The disclosed results are analogous with the previous finding of Wei and co-workers [32]. The surfactants that have good solubilising capacity for drugs may not be equally effective for solubilising the oil phase. Thus, the selection of surfactant or co-surfactant was further governed by their ability to nanoemulsify the 1 : 1 mixture of selected oil and water rather than considering solubilisation capacity of CVD solely.

3.2. *Screening of surfactants for nanoemulsifying ability*

In formulation of NEs that will be used as drug delivery systems, it is very important to determine with which oil a given surfactant forms NE. Thus, nanoemulsification ability (S_{min}) of various surfactants was determined against different oils (Table 2). Miglyol 810® required 46.52% w/w of Acconon CC6® for nanoemulsification of equal mixture of oil and water (Table 2), whereas a mixture of Labrafil M 1944CS® and water (1 : 1) obligated 54.05% w/w and 54.55% w/w of Labrasol® and Acconon CC6®, respectively, for nanoemulsification. Tween 80 has shown a good solubilising ability for Capmul PG8® mixture (37.5% w/w). Acconon CC6® has shown the best nanoemulsifying ability (S_{min} 46.52% w/w) for Miglyol 810® and also shown a good solubility for CVD (44.32 ± 6.89 mg/mL), whereas 60.94% w/w Labrasol® and 63.63% w/w Tween 80 was required for emulsification of Miglyol 810® (Table 2). Extremely high surfactants concentration (>80%) was required for emulsification of both olive oil and oleic acid that could be due to high long-chain fatty acid content in said oils [33]. On the other hand, Miglyol 810® which is a caprylic/capric acid triglyceride is emulsified easily by Acconon CC6® and requires least surfactants concentration (46.52% w/w) among the selected oils. MCTs contain about 95% of fatty acids which are made up of C8-C10 carbon atoms, and therefore they also have molecular volume less than long-chain triglycerides. The results are very well corroborated with earlier reports that oils consisting of short-chain fatty acid

Table 2. The surfactant nanoemulsification efficiency (S_{min}) and percentage transmittance for oils investigated after 24 h.

	Surfactants					
	Labrasol®		Acconon CC6®		Tween 80	
Oils	S_{min} (%)	Transmittance (%)	S_{min} (%)	Transmittance (%)	S_{min} (%)	Transmittance (%)
Labrafil M1944®	54.05	99.32	54.55	99.47	76.47	95.72
Labrafil M2125®	60.00	98.45	55.55	99.39	77.27	94.87
Oleic acid	78.72	93.02	73.33	94.57	69.23	96.81
Capmul PG8®	75.00	94.31	59.54	98.66	37.50	99.37
Miglyol 810®	60.94	97.73	46.52	99.71	63.63	97.32
Olive oil	90.00	78.94	83.60	80.05	–	–

could be solubilsed/emulsified to a greater extent by non-ionic surfactants than the oils of longer chain fatty acids [33,36]. In contrast, Labrasol® and Tween 80 are less efficient surfactants for Miglyol 810®. The variation may be due to varying chain length and structure of surfactants [37]. Interestingly, Labrafil M1944CS® and Labrafil M2125CS® an oleyl and linoleyl polyoxylglycerides (esters of long-chain fatty acids), respectively, are solubilised easily by Labrasol® and Acconon CC6®, even though they are long-chain fatty acids composition. This could be attributed to their chemical structure and co-emulsifying property of oil. These results were further substantiated by measuring the % transmittance of nanoemuslion obtained on titration of oil/water mixture (1 : 1) with various surfactants. The percentage transmittance values of various NE dispersion are given in Table 2. The study revealed that Acconon CC6® as a surfactant with Miglyol 810® (as oil) showed best transmittance (99.71%) at lowest S_{min} value (46.52% w/w) in comparison to other studied surfactants and was selected for further investigation.

3.3. *Screening of co-surfactants*

In most cases, single-chain surfactants alone are unable to reduce the oil/water interfacial tension sufficiently to enable a NE to form. Medium-chain length alcohols, which are commonly added as co-surfactants, have the effect of further reducing the interfacial tension, whilst increasing the fluidity of the interface thereby increasing the entropy of the system [21]. A medium-chain length alcohol also increases the mobility of the hydrocarbon tail and also allows greater penetration of the oil into this region. Despite advantages of the use of medium-chain alcohol as co-surfactant, they are not suitable for pharmaceutical preparations due to their high irritation potential. Therefore, co-surfactants selected for study were Plurol Oleique® Cremophore RH40®, CO-20®, Labrasol®, Transcutol P® and ethanol. Two criteria were set for selection of co-surfactants (i) improvement in nanoemulsification ability (S/CoS_{min}) of Acconon CC6® and (ii) existence of NE region at 1 : 1 ratio of surfactant/co-surfactants mixture. The minimum amount of Acconon CC6®/co-surfactants (S/CoS_{min}) mixture required to produce NEs was determined by titrating oily mixture (Miglyol 810® + water, 1 : 1) with an equal mixture of Acconon CC6®/co-surfactants, and the results obtained are presented in Table 3.

Table 3. The co-surfactants nanoemulsification efficiency (S/CoS_{min}) and percentage transmittance for Miglyol 810® oils after 24 h.

Co-surfactants	HLB[a]	S/CoS_{min}[b] (%)	Transmittance (%)
CO-20®	11.50	37.11	99.64
Plurol Oleique®	11.25	41.18	95.45
Labrasol®	13.25	45.94	96.31
Cremophore RH40®	13.50	40.37	96.82
Ethanol	–	60.94	95.72
Transcutol P®	8.25	73.19	96.32

Note: [a]HLB for equal mass mixture of Acconon CC6® and co-surfactants.
[b]Minimum S/CoS mixture (at 1 : 1 ratio) required for solubilisation of equal mass mixture of Miglyol 810® and water.

CO-20®, Plurol Oleique®, Labrasol® and Cremophore RH40® improved the nanoemulsifying ability of Acconon CC6®, but Labrasol® still did not work efficiently and there was no significant difference in the nanoemulsifying ability compared to the co-surfactant free system. Whereas, CO-20®, Plurol Oleique® and Cremophore RH40® improved the nanoemulsifying efficiency of surfactant, and $S/\mathrm{Co}S_{\min}$ values were found to be 37.11% w/w, 41.18% w/w and 40.37% w/w, respectively (Table 3). It is generally accepted that high HLB (8–18) surfactants and/or surfactant mixtures favour the formation of o/w NE systems. In this study, HLB values of Acconon CC6® with other co-surfactants (Table 3) revealed that HLB concept is not quite applicable for efficient working of surfactant mixture, as Acconon CC6®/CO-20® worked quite efficiently even though the HLB value 11.5 is less than the Acconon CC6®/Labrasol® (13.25) and Acconon CC6®/Cremophore RH40® (13.5) mixture. This may be due to the fact that the raw materials used for synthesis of surfactants are usually mixtures of fatty acids with different hydrocarbon chain lengths and fraction of un-reacted polyoxyethylene, polyglycerol and ethoxyls which may influence their nanoemulsifying efficiency [38,39]. In addition, variation in chemical structure of these non-ionic surfactants could be another factor for influencing the nanoemulsifying efficiency of co-surfactants.

In contrast, ethanol and Transcutol P® further reduced the Acconon CC6® nanoemulsifying efficiency. $S\mathrm{Co}S_{\min}$ values of the Acconon CC6®/Transcutol P® and Acconon CC6®/ethanol mixtures were found to be 60.94% w/w and 73.19% w/w, respectively (Table 3). The decreased nanoemulsifying efficiency of Acconon CC6® could be due to the excellent solvent property of ethanol and Transcutol P® (diethylene glycol monoethyl ether), which modify the microenvironment of Acconon CC6® and lead to the reduced solubilisation capacity for oil and water phases. Similar results were reported with Labrasol® (surfactant) and Transcutol P® (co-surfactant) mixture at varying mass ratios. Solubilisation efficiency of Labrasol® was further decreased on increasing the contents of Transcutol P® [40].

In order to substantiate the selection of co-surfactant, the NE existence region was considered as another criterion. The pseudo-ternary phase diagrams were developed using Miglyol 810® as oil, Acconon CC6® as surfactant with different co-surfactants at ratio 1 : 1 and compared for NE existence area (Figure 1). Surfactant mixture Acconon CC6®/CO-20® (HLB = 11.5) showed maximum NE region (Figure 1(e)), followed by Acconon CC6®/Cremophore RH40® (HLB = 13.5) (Figure 1(d)) and Acconon CC6®/Labrasol® (HLB = 13.25; Figure 1(c)). Whereas, Acconon CC6®/Plurol Oleique® (HLB = 11.25) (Figure 1(b)) and Acconon CC6®/Transcutol P® (HLB = 8.25) (Figure 1(a)) showed significantly less NE existence region in comparison to surfactant (Acconon CC6®) alone (Figure 2(a)). The presence of a high NE region using CO-20® as co-surfactant with Acconon CC6® could be due to its high solubilisation efficiency ($S\mathrm{Co}S_{\min}$ = 37.11% w/w) as discussed before. In contrast, ethanol did not work as a co-surfactant with Acconon CC6® and no NE region was observed at $S/\mathrm{Co}S$ ratio 1 : 1. Whereas, use of Acconon CC6®/Transcutol P® reduced the NE existence region in comparison to co-surfactant free phase diagram (Figures 1(a) and 2(a)). The finding confirms the results obtained earlier that the combination of Transcutol P® with surfactant (Acconon CC6®) decreased the nanoemulsifying efficiency. Thus, the presence of different types of co-surfactants can affect the phase behaviour of NE. Consequently, the above results support the selection of CO-20® as an efficient co-surfactant for

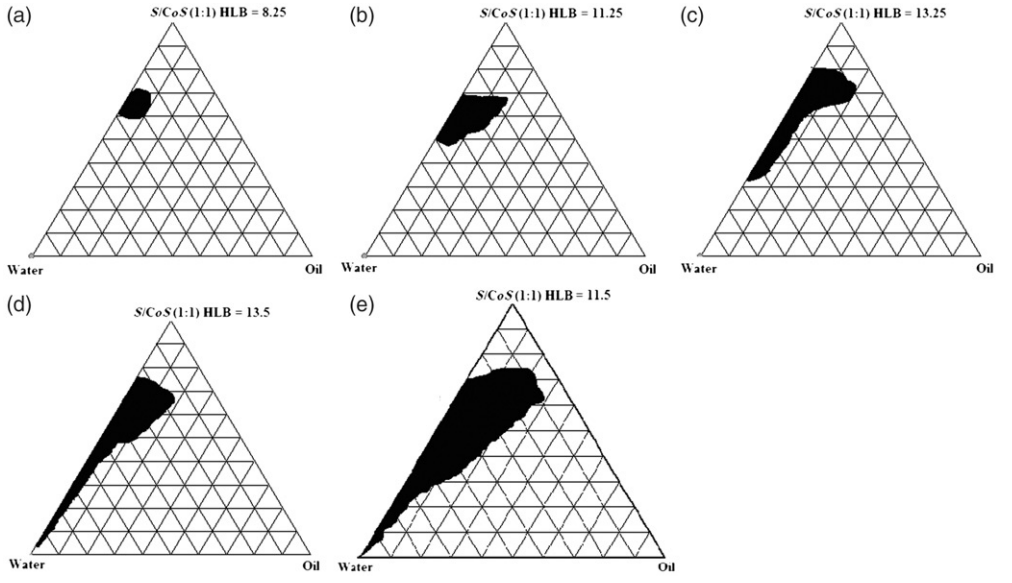

Figure 1. Pseudo-ternary phase diagrams showing nanoemulsion existence range composed of Miglyol 810® (oil), Acconon CC6® (surfactant), water and different co-surfactants. (a) Transcutol P®; (b) Plurol Oleique®; (c) Labrasol®; (d) Cremophore RH40®; and (e) CO-20® at *S*/Co*S* 1 : 1 ratio.

development of NE using Miglyol 810® and Acconon CC6® for transdermal delivery of CVD.

3.4. *Construction of pseudo-ternary phase diagrams*

Pseudo-ternary phase diagrams were constructed to find out the concentration range of components for the existence range of NEs by aqueous titration method at ambient temperature. Phase diagrams were constructed by using Miglyol 810® as an oil phase and Acconon CC6®/CO-20® at different *S*/Co*S* ratios (1 : 0, 1 : 1, 1 : 2, 1 : 4, 2 : 1 and 4 : 1) and presented in the Figure 2. The dark area in the phase diagram shows NE (single phase) existence region, rest of the area on the phase diagram represents the turbid and conventional emulsions (Figure 2). The percentage of existence area of NE at different *S*/Co*S* ratios is presented in Figure 3.

In the absence of co-surfactants, Acconon CC6® [Figure 2(a) (*S*/Co*S* ratio 1 : 0)] was able to form NE over a short range of surfactant–oil–water ratios (Figure 2(a)). The NE existence region occupied about 4.81% of the total existence area of the pseudo-ternary phase diagram (Figure 3). A very low amount of oil (10% w/w) could be solubilised at a very high concentration of surfactant mixture and which could solubilise a maximum of 40% water. The low NE area and less oil solubilsation at *S*/Co*S* 1 : 0 could be probably attributed to inefficiency of surfactant to reduce the interfacial tension in absence of co-surfactant. On addition of co-surfactant to surfactant in equal amount (*S*/Co*S* ratio 1 : 1), the NE area in the phase diagram increased significantly to 21.86% (Figure 3). The oil could be solubilised up to 29% w/w at a relatively low surfactant mixture concentration

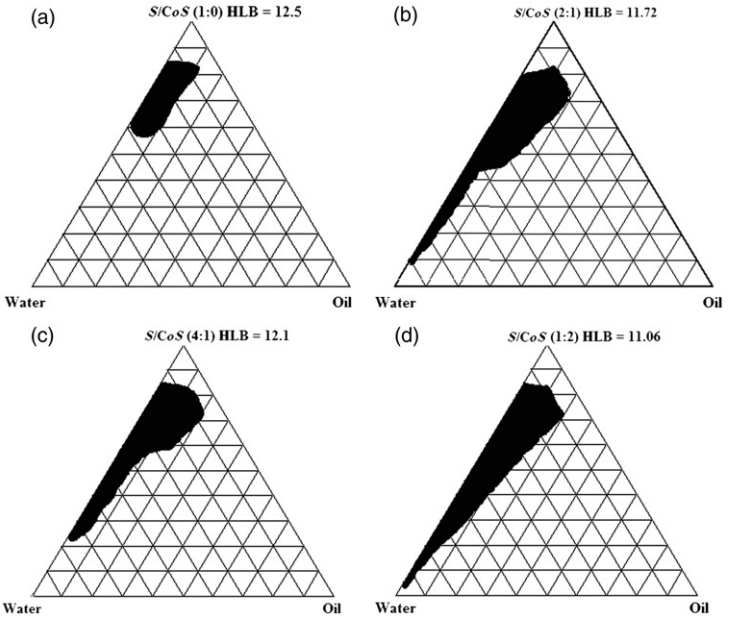

Figure 2. Pseudo-ternary phase diagrams showing nanoemuslion existence range composed of Miglyol 810® (oil), Acconon CC6® (surfactant), CO-20® (co-surfactant) and water at different *S*/Co*S* ratios.

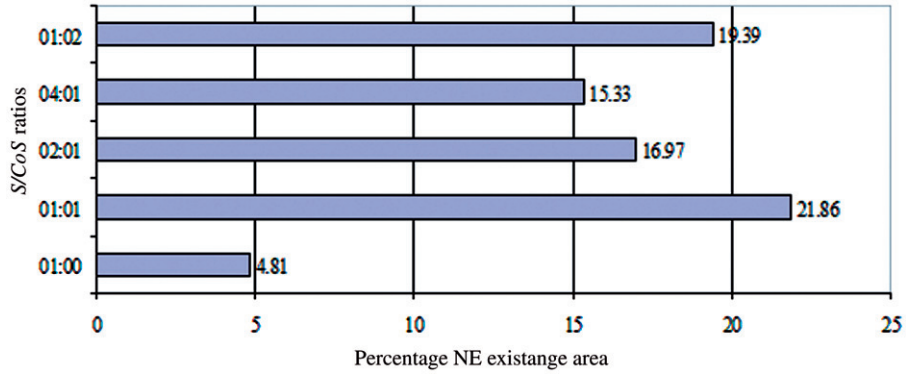

Figure 3. Nanoemulsion existence area obtained with Acconon CC6® as surfactant and CO-20® as co-surfactant at different *S*/Co*S* ratios in the pseudo-ternary phase diagrams.

of 62% w/w (Figure 1(e)). On further increase in co-surfactant content to make *S*/Co*S* ratio 1 : 2, NE area was decreased to 19.39% of total existence area, which is not significant as compared to area obtained at *S*/Co*S* ratio 1 : 1 ratio ($p > 0.05$) (Figure 2(d)). The NE at *S*/Co*S* ratio 1 : 2 showed high viscosity, and also observed gel region in phase diagram (not shown in figure). At *S*/Co*S* ratio 1 : 4, very few NEs were found which were viscous, unstable, turned turbid on dilution and showed phase separation after 24 h

(phase diagram not shown). Gel region was observed at high co-surfactants content; these gels were toughened on addition of water, however broken down on further dilution with water before transformation into coarse emulsion. Thus, it could be concluded that on increasing the co-surfactant content, NE existence region decreases progressively, and more unstable gel was observed at high co-surfactant content.

On increase in surfactant content with respect to co-surfactant [*S*/Co*S* ratio 2 : 1] (Figure 2(b)), NE region was decreased in comparison to region obtained at SCoS ratio 1 : 1. About 20% w/w of oil could be solubilised with a surfactant mixture concentration of 72% w/w (Figure 2(b)) and the NE area obtained was 16.97% of the total area of the pseudo-ternary phase diagram (Figure 3). When the surfactant concentration was further increased to four parts to one part of co-surfactant (Figure 2(c)), the NE area (15.33%) decreased and maximum of 19% w/w of oil could be solubilised at 72% w/w *S*/Co*S* value. NE obtained at *S*Co*S* ratios 1 : 1, 2 : 1 and 1 : 2 can be diluted with water to a greater extent in comparison to others as shown in Figures 1(e) and 2(b)–(d).

The surfactant and co-surfactant mass ratio has been found as a key factor that influenced the phase properties and existence of NE region. It could be observed that increase in content of both surfactant and co-surfactant decreased the NE region in phase diagram (Figure 2). The maximised NE region was observed at *S*/Co*S* ratio 1 : 1 with highest oil solubilisation (29% w/w) at a relatively low surfactant mixture of 62% w/w. Probably, CO-20® (PEG-20 castor oil) at equal mixture with Acconon CC6® forms more flexible surfactant/co-surfactant interfacial film, which determines the existence of NE region [41]. Similar observation was reported previously that at equal mass ratio of surfactant/co-surfactant mixture maximised NE region which could be attributed to maximum oil solubility at optimum surfactant/co-surfactant ratio [23].

3.5. *Selection of nanoemulsion formulations*

It is well known that the content of oil and surfactant mixture always affects the skin permeation of drug as well as other physical parameters of NE [15,16,23]. For transdermal delivery, maximised skin permeation is the primary aim; hence, NE formulations were selected in such a way that could give maximum skin permeation at minimum possible surfactant concentration. Thus, NEs with varying oil (10–20% w/w) and *S*/Co*S* (35–50% w/w, 1 : 1 ratio) concentration were prepared to study the effect of oil and surfactants on skin permeation rate. One millilitre of each NE formulation loaded with 2.5 mg of CVD was taken for different studies.

3.6. *Characterisation of nanoemulsions*

Emulsions are thermodynamically unstable and eventually phase separated on stress testing, such as centrifugation, freeze thaw cycle and even storing for a long period. Thus, to evaluate the stability of NEs and to identify and avoid the metastable system, centrifugation and freeze thaw stability studies were performed. The formulations that survived the above tests were selected for further studies, and the compositions of the selected NEs are presented in Table 4.

The droplet size of CVD-loaded NE vesicles was small with all the formulations having a mean vesicle size between 9.28 and 95.47 nm (Table 4). The NE formulation F2

Table 4. Nanoemulsion composition selected from pseudo-ternary phase diagram of *S*/Co*S* ratio 1 : 1 and the data for evaluation parameters like mean globules size, polydispersity index (PI), viscosity, refractive index (RI), pH and percentage transmittance.

Formulation	Oil (% w/w)	*S*/Co*S* (% w/w)	Water (% w/w)	Mean globules size (nm)	PI	Viscosity (cps)	RI	pH	Transmittance (%)
F1	10	50	40	11.32	0.118	54.83 ± 5.39	1.417 ± 0.008	6.5 ± 0.51	99.32
F2	12.5	50	37.5	9.28	0.103	58.07 ± 4.82	1.411 ± 0.011	6.4 ± 0.42	99.30
F3	15	50	35	21.54	0.137	59.64 ± 6.22	1.422 ± 0.010	6.0 ± 0.31	99.27
F4	17.5	50	32.5	84.94	0.298	81.34 ± 8.47	1.432 ± 0.011	5.8 ± 0.27	98.17
F5	20	50	30	95.47	0.319	105.76 ± 12.83	1.441 ± 0.012	5.6 ± 0.51	96.02
F6	10	45	45	23.7	0.209	57.18 ± 4.27	1.406 ± 0.009	5.8 ± 0.38	99.12
F7	10	40	50	25.82	0.202	53.07 ± 4.62	1.403 ± 0.011	5.9 ± 0.41	99.18
F8	10	35	55	36.27	0.238	34.83 ± 4.22	1.404 ± 0.015	5.6 ± 0.19	98.29

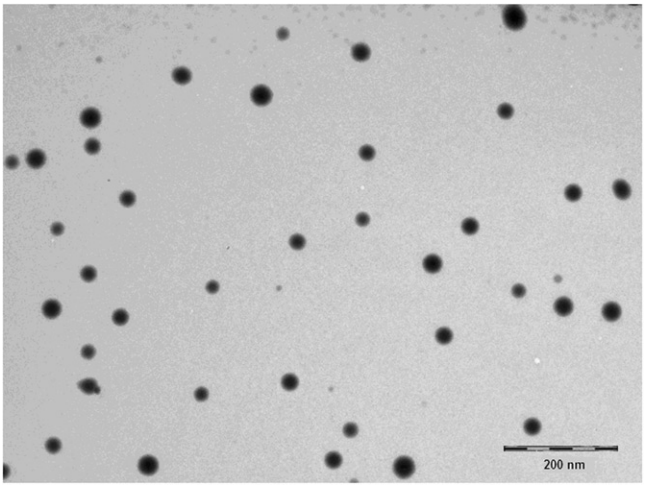

Figure 4. Micrograph of carvedilol nanoemulsion under transmission electron microscope (TEM).

containing 12.5% w/w oil and 50% *S*/Co*S* w/w showed lowest mean globules size and PI 0.103 (Table 4). Insignificant difference in mean globules was observed by slight increase in oil contents from 10 to 12.5% w/w ($p > 0.05$). However, on further increase of oil content up to 20% w/w, significant increase in mean size was observed ($p < 0.05$) (Table 4). The results presented are in agreement with the previous report that reveals a directly proportional relationship between oil concentration and mean globules size [12,42]. Similar findings were reported by Yuan and associates [23], that the increase in IPM as oil from 5% to 15% w/w, globules size of meloxicam-loaded microemulsion was correspondingly increased. The significantly increased globules size with increasing oil concentration could be attributed to expansion of oil droplets of NE by further addition of the oil [43,44]. In contrast, mean globules size of NEs decreases on increasing *S*/Co*S* concentration at fixed oil content (10% w/w) (Table 4), which might be explained that increase in *S*/Co*S* concentration reduce the interfacial tension of oil and water.

A transmission electron microscopic (TEM) observation of the CVD NEs was made immediately after the preparation, and the resultant micrograph is presented in Figure 4. The droplet on the NE appears dark with the bright surroundings. TEM photographs further confirmed that the globules are spherical in shape and also substantiate the results of globules size obtained in droplet size analysis.

Viscosity of nanoemuslion imparts a direct correlation with oil and surfactant concentration at constant *S*/Co*S* ratio (1 : 1) (Table 4). The study showed that viscosity increases on using high proportion of oil for the nanoemuslion preparation, and that relation was apparent when the Miglyol 810® content was increased from 15 to 20% w/w (F3–F5) at fixed *S*/Co*S* content ($p < 0.05$). Similarly, it was decreased on reducing the surfactant mixture concentration. It is obvious that the average droplet size, viscosity and refractive index of NEs with more oil and surfactant increased significantly. Low refractive index (1.403–1.432) (Table 4) values of all NE indicate its isotropic nature.

Transmittance studies using double-beam UV-VIS spectrophotometer were performed to further substantiate the isotropic nature of NE. All NEs were clear and transparent as

shown by the high values of percentage transmittance (Table 4). Though their value was slightly dipped to 96.02% at high Miglyl 810® concentration (20% w/w). The pH values (5.6–6.5) were within the physiological range of skin (Table 4).

3.7. Ex vivo *skin permeation studies*

Selected NEs were evaluated for permeation efficiency through wistar rat skin. The excised wistar rat skin was used as the model membrane because the rat skin has more structural similarities to human tissue, and also permeation kinetic parameters are comparable with human skin [6]. The effect of concentration of oil and *S*/Co*S* (1 : 1) on the skin permeation of CVD was evaluated across rat skin and shown in Figures 5 and 6. The permeation

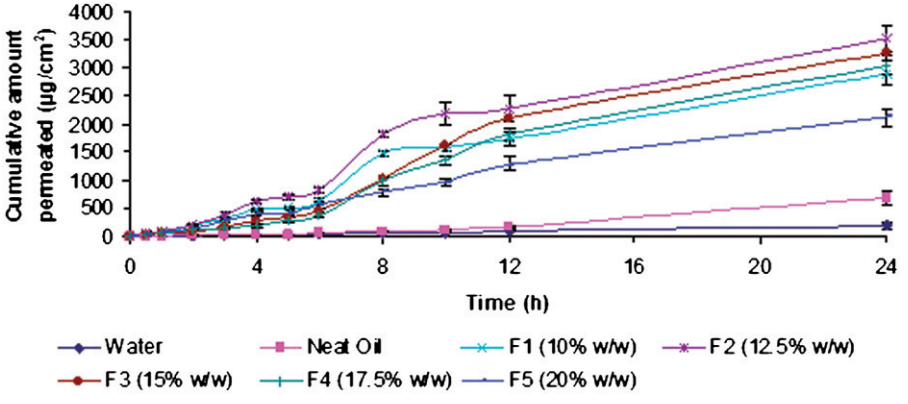

Figure 5. The effect of amount of oil present in nanoemulsion on the permeation rate of carvedilol (mean value ± SD; $n = 3$).

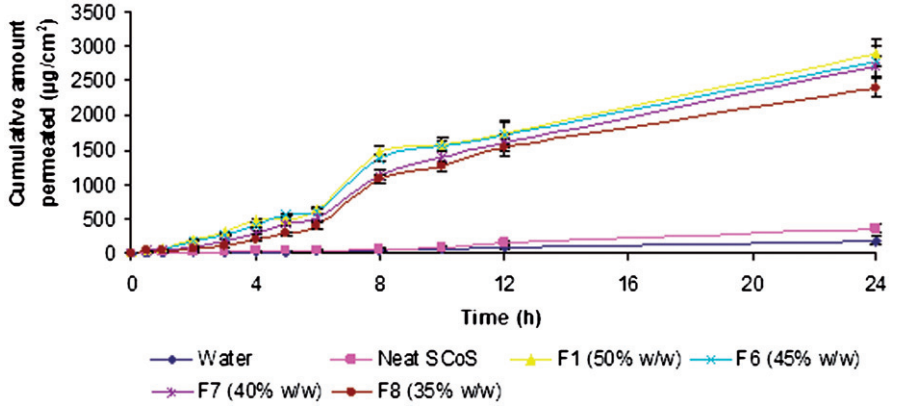

Figure 6. The effect of amount of mixture of surfactants (*S*/Co*S*, 1 : 1) in nanoemulsions on the permeation rate of carvedilol (mean value ± SD; $n = 3$).

parameters including the cumulative amount at 24 h, flux (F), permeability coefficient (Pb), enhancement ratio (ER) and lag time (T_{lag}) were calculated and listed in Table 5.

The content of oil at fixed S/CoS concentration played an important role in NE formulation, and it also affects the skin permeation rate directly. Figure 5 shows the effect of the content of Miglyol 810® as oil ranged from 10 to 20% w/w on the skin permeation of CVD, while the content of surfactant and co-surfactant mixture S/CoS (1 : 1) was kept constant at 50% w/w. As the content of oil increased from 12.5 to 20% w/w (F2–F5), the skin permeation rate of CVD decreased from 161.53 ± 23.65 to $92.251 \pm 38.54\,\mu g/cm^2/h$. The highest permeation rate at 12.5% w/w oil content (formulation F2) could be substantiated to small globules size and low viscosity of the formulation. Presence of small globules makes better chance to adhere to skin membrane and hence enhances the skin penetration of drug molecules than the larger globules of NE. It may be concluded that the presence of droplets in size of several nanometres had significant contribution to the percutaneous penetration of CVD and consequently influence the lag time. Effect of mean globules size of NE on flux and lag time is presented in Figure 7. The results presented here are inconsistent with previous findings that on increasing the oil content from 5 to 15%, fluxes of meloxicam were significantly decreased due to large globules size of microemulsion [23]. Sintov and Shapiro [45] studied the effect of vehicles on lidocaine permeation across mouse skin. Lidocaine-loaded microemulsion as vehicle was compared with lidocaine in oil-free micellar system, and lidocaine in a mixture of the surfactants and the co-surfactants for skin permeation efficiency. They disclosed that lidocaine fluxes were found highest with micoemulsion as vehicle in comparison to other selected vehicle. High flux obtained using micoemulsion could be due to the presence of droplets of oil in nanosize range in microemulsion [45]. In addition to the size of NE, viscosity may also decrease considerably the skin permeation of the drug across skin [46], and thus

Table 5. Percutaneous permeation parameters of the nanoemulsion formulations across wistar rat skin.

Formulations	Cumulative amount ($\mu g/cm^2$)[a]	Flux ($\mu g/cm^2/h$)[a]	Pb (10^3 cm/h)[a]	ER[b]	T_{lag} (h)
Water	189.34 ± 71.71	7.88 ± 1.21	3.15 ± 0.32	–	4.2 ± 0.78
Neat oil	670.51 ± 112.66	26.02 ± 2.29	10.41 ± 0.61	–	3.0 ± 0.56
Neat S/CoS	371.79 ± 61.35	14.87 ± 1.81	5.95 ± 0.65	–	3.2 ± 0.44
F1	2897.47 ± 213.42	130.40 ± 22.64	52.16 ± 4.12	5.0 ± 0.87	0.7 ± 0.010
F2	3516.33 ± 221.11	161.53 ± 23.65	64.61 ± 6.73	6.2 ± 1.21	0.5 ± 0.010
F3	3255.08 ± 312.29	149.15 ± 37.27	59.66 ± 5.18	5.7 ± 1.13	1.2 ± 0.021
F4	3040.94 ± 176.63	136.82 ± 33.65	54.73 ± 4.77	5.3 ± 0.91	1.5 ± 0.022
F5	2114.38 ± 191.26	92.251 ± 38.54	36.90 ± 6.39	3.5 ± 1.47	1.8 ± 0.029
F6	2781.84 ± 214.44	126.23 ± 21.83	50.49 ± 3.78	4.9 ± 0.89	0.2 ± 0.010
F7	2711.18 ± 151.71	122.65 ± 22.37	49.06 ± 6.18	4.7 ± 1.21	0.5 ± 0.011
F8	2402.82 ± 131.77	111.32 ± 23.26	44.53 ± 5.41	4.3 ± 1.22	0.5 ± 0.012

Notes: mean ± SD; $n = 3$.

[a]Data for formulation F1–F8 is statistically significant ($p < 0.05$) in comparison with control vehicles (water, neat oil and neat S/CoS).

[b]Enhancement ratio (ER) for formulation F1–F8 in comparison to neat oil as control and were found significant ($p < 0.05$).

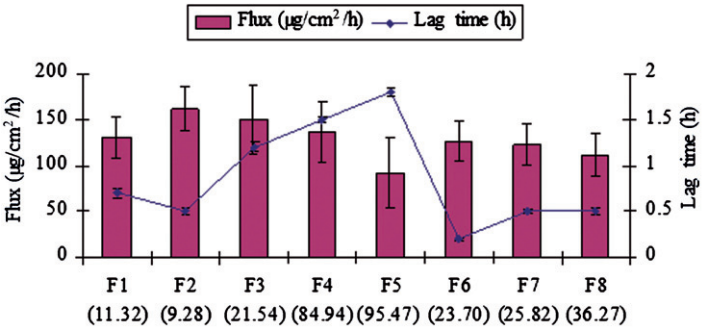

Figure 7. A comparative profile showing effect of mean globules size on skin permeation rate (flux) and on lag time (mean globule size presented in parenthesis of nanoemulsion formulation coded on *x*-axis).

consequently increased the lag time from 0.5 to 1.8 h (Table 5). NE formulation containing 10% w/w oil (F1) showed lesser permeation rate and equivalent lag time in comparison to 12.5% w/w oil containing formulation (F2). This could be due to slight penetration promoting properties of Miglyol 810® oil, which showed additional influence on skin penetration at 12.5% w/w oil content [47].

Surfactant mixture, which played a significant role in preparation of NE also, has been shown to affect the skin permeation rate. To study this effect, the oil content was kept constant at 10% w/w, the formulation F1, F6, F7 and F8 in which the contents of surfactant mixture were 50, 45, 40 and 35% w/w (S/Co$S = 1:1$), respectively, were investigated for skin permeation rate (Figure 6). The skin permeation rate data are calculated and listed in Table 5. As the content of S/CoS (1 : 1) decreased from 50% w/w to 35% w/w at fixed oil content (10% w/w) the permeation rate of CVD correspondingly reduced from 130.40 ± 22.64 to $111.32 \pm 23.26\,\mu g/cm^2/h$ (Figure 6, Table 4). The decrease of flux is not prominent on decreasing the surfactant mixture to 40% w/w ($p > 0.05$); however, it decreased significantly by reducing S/CoS to 35% w/w. The result obtained here is in contrast to previous hypothesis that on increasing the content of surfactants mixture, the permeation rate across rat skin usually decreases due to decrease in thermodynamic activity of drug [16,23,48]. The results do not follow the general trend, which could be owing to better interaction of small droplets of oil with SC which was achieved at a high amount of surfactant mixture. The small droplets settled down to close contact with skin and a large amount of drugs from oil in NE could be penetrated across skin [44]. In addition, previous data suggests that permeation rate decreases at a very high concentration of surfactant mixture (more that 50%), and high oil with high surfactant content in NE may synergistically affect the skin permeation rate [23,48]. Similarly, high permeation rate for microemulsion containing large amount of surfactant was reported by Baroli and co-workers [49] for topical delivery of 8-methoxsalen. They suggested that high fluxes obtained might be explained by permeation enhancing effects of microemulsion components [49]. The skin permeation rate for all NE formulations were significantly higher than the drug in water, neat oil and neat S/CoS ($p < 0.05$). The ER of each NE was 6.2–3.5-fold higher than the neat oil ($p < 0.05$) and also lag time decreased significantly up to 0.5 h in comparison to control (3.2–4.2 h).

The maximum flux obtained through rat skin is $161.53 \pm 23.65\,\mu g/cm^2/h$ from NE formulation F2 having 12.5% w/w oil and 50% w/w S/CoS at 1 : 1 ratio. According to Flynn and Stewart (1988) [50], the predictive maximal (C) concentrations of drug that would penetrate human skin after topical application can be calculated from $C = J_{max}.A/Cl_p$.[43] Where, J_{max} is the maximum flux determined, A is the area of application and Cl_p the plasmatic clearance. The calculated maximum plasma (C) concentration following the application of F2 NE formulation on human skin of area $100\,cm^2$ would achieve $0.45\,\mu g/ml$. The maximum plasma concentration is calculated using reported value of Cl_p (600 ml/min) [3]. The calculated maximum plasma concentration is sufficient to achieve therapeutic concentration for sustained action of drug.

4. Conclusions

NE vehicles for enhanced and sustained transdermal delivery of CVD were developed using Miglyol 810® as oil, Acconon CC6® and CO-20® as surfactant and co-surfactant, respectively. The components for NE were selected on the basis of high solubilisation capacity of drug, nanoemulsifying ability of surfactants and area of NE region in phase diagram. The selected NEs from pseudo-ternary phase diagrams were finally optimised for high flux by *in vitro* skin permeation studies. All the NE showed significantly high fluxes of CVD across rat skin as compared to neat components ($p < 0.05$). The flux obtained during in vitro skin permeation studies is sufficiently high to achieve therapeutic drug level in human beings for 24 h for sustained management of hypertension. The maximum plasma concentration of $0.45\,\mu g/ml$ could be achieved using NE is predicted by mathematical calculation.

Acknowledgements

The authors would like to thank Colorcon Asia Pvt. Ltd., (Mumbai, India); Abitec Corporation (Janesville, WI, USA); and Nikko Chemicals (Japan) for kindly supplying the samples of oil and surfactants used in this study. The authors are also thankful to All India Institute of Medical Science (AIIMS) for TEM study. This work was financially supported by the University Grants Commission (UGC), New Delhi, under RFSMS scheme (#F. 4-3/2006 (BSR)/11-26/2008 (BSR).

References

[1] L.Y. Galichet (ed.), *Clarke's analysis of drug and poisons*. Available at https://www.medicinescomplete.com/mc/clarke

[2] C. Dollery, *Therapeutic Drugs*, 2nd ed., Vol. 1, Churchill Livingstone, New York, 1999, pp. 115–118.

[3] Prescription Information COREG® (carvedilol) tablets, GlaxoSmithKline. Available at http://us.gsk.com/products/assets/us_coreg.pdf

[4] R.C. Mundargi, S.A. Patil, and T.M. Aminabhavi, *Evaluation of acrylamide-grafted-xanthan gum copolymer matrix tablets for oral controlled delivery of antihypertensive drugs*, Carbohydr. Polym. 69 (2007), pp. 30–141.

[5] C. Wei, K.A. Lamey, J. Malofy and C. Oh. Carvedilol Formulations, King of Prussia PA. US Patent Application 20050261335 A1 (2005).

[6] B. Godin and E. Touitou, *Transdermal skin delivery: Prediction for humans from* in vivo, ex vivo *and animal models*, Adv. Drug Deliv. Rev. 59 (2007), pp. 1152–1161.
[7] A.C. Williams and B.W. Barry, *Penetration enhancers*, Adv. Drug Deliv. Rev. 56 (2004), pp. 603–618.
[8] W.I. Higuchi, S.K. Li, G. Abdel-Halim, H. Zhu, and Y. Song, *Mechanistic aspects of iontophoresis in human epidermal membrane*, J. Control Release 62 (1999), pp. 13–23.
[9] S. Mitragotri and J. Kost, *Low frequency sonophoresis: A review*, Adv. Drug Deliv. Rev. 56 (2004), pp. 589–601.
[10] G. Cevc, *Lipid vesicles and other colloids as drug carriers on the skin*, Adv. Drug Deliv. Rev. 56 (2004), pp. 675–711.
[11] M.M.A. Elsayed, O.Y. Abdallah, V.F. Naggar, and N.M. Khalafallah, *Deformable liposomes and ethosomes: Mechanism of enhanced skin delivery*, Int. J. Pharm. 322 (2006), pp. 60–66.
[12] A. Azeem, M. Rizwan, F.J. Ahmad, Z. Iqbal, R.K. Khar, M. Aqil, and S. Talegaonkar, *Nanoemulsion components screening and selection: A technical note*, AAPS Pharm. SciTech. 10 (2009), pp. 69–76.
[13] P.J. Lee, R. Langer, and V.P. Shastri, *Novel microemulsion enhancer formulation for simultaneous transdermal delivery of hydrophilic and hydrophobic drugs*, Pharm. Res. 20 (2003), pp. 264–269.
[14] D. Mou, H. Chen, D. Du, C. Mao, J. Wan, H. Xu, and X. Yang, *Hydrogel-thickened nanoemulsion system for topical delivery of lipophilic drugs*, Int. J. Pharm. 353 (2008), pp. 270–276.
[15] Y.B. Huang, Y.H. Lin, T.M. Luc, R.J. Wang, Y.H. Tsai, and P.C. Wu, *Transdermal delivery of capsaicin derivative-sodium nonivamide acetate using microemulsions as vehicles*, Int. J. Pharm. 349 (2008), pp. 206–211.
[16] X. Zhao, J.P. Liu, X. Zhang, and Y. Li, *Enhancement of transdermal delivery of theophylline using microemulsion vehicle*, Int. J. Pharm. 327 (2006), pp. 58–64.
[17] G.M. El Maghraby, *Transdermal delivery of hydrocortisone from eucalyptus oil microemulsion: Effects of cosurfactants*, Int. J. Pharm. 355 (2008), pp. 285–292.
[18] W. Zhu, A. Yu, W. Wang, R. Dong, J. Wu, and G. Zhai, *Formulation design of microemulsion for dermal delivery of penciclovir*, Int. J. Pharm. 360 (2008), pp. 184–190.
[19] X. Wang, Y. Jiang, Y.-W. Wang, M.-T. Huang, C.-T. Hoa, and Q. Huang, *Enhancing anti-inflammation activity of curcumin through O/W nanoemulsions*, Food Chem. 108 (2008), pp. 419–424.
[20] A. Kogan and N. Garti, *Microemulsions as transdermal drug delivery vehicles*, Adv. Drug Deliv. Rev. 123 (2006), pp. 369–385.
[21] M.J. Lawrence and G.D. Rees, *Microemulsion-based media as novel drug delivery systems*, Adv. Drug Deliv. Rev. 45 (2000), pp. 89–121.
[22] S. Peltola, P. Saarinen-Savolainen, J. Kiesvaara, T.M. Suhonen, and A. Urtti, *Microemulsions for topical delivery of estradiol*, Int. J. Pharm. 254 (2003), pp. 99–107.
[23] Y. Yuan, S.-M. Li, F.-K. Mo, and D.-F. Zhong, *Investigation of microemulsion system for transdermal delivery of meloxicam*, Int. J. Pharm. 321 (2006), pp. 117–123.
[24] C. Mohammed and V. Manoj, *Aerosol-OT microemulsions as transdermal carriers of tetracaine hydrochloride*, Drug Dev. Ind. Pharm. 26 (2000), pp. 507–512.
[25] Y.S. Tanwar, C.S. Chauhan, and A. Sharma, *Development and evaluation of carvedilol transdermal patches*, Acta Pharm. 57 (2007), pp. 151–159.
[26] U. Ubaidulla, M.V. Reddy, K. Ruckmani, F.J. Ahmad, and R.K. Khar, *Transdermal therapeutic system of carvedilol: Effect of hydrophilic and hydrophobic matrix on* in vitro *and* in vivo *characteristics*, AAPS PharmSciTech. 19 (2007), pp. E1–E8.
[27] N. Dixit, K. Kohli, and S. Baboota, *Nanoemulsion system for the transdermal delivery of a poorly soluble cardiovascular drug*, PDA J. Pharm. Sci. Technol. 62 (2008), pp. 46–55.

[28] B. Sapra, S. Jain, and A.K. Tiwary, *Transdermal delivery of carvedilol in rats: Probing the percutaneous permeation enhancement mechanism of soybean extract-chitosan mixture*, Drug Dev. Ind. Pharm. 35 (2009), pp. 230–241.
[29] B. Sapra, S. Jain, and A.K. Tiwary, *Effect of* Asparagus racemosus *extract on transdermal delivery of carvedilol: A mechanistic study*, AAPS Pharm. Sci. Tech. 10 (2009), pp. 199–210.
[30] R. Gannu, Y.V. Vishnu, V. Kishan, and Y.M. Rao, In vitro *permeation of carvedilol through porcine skin: Effect of vehicles and penetration enhancers*, PDA J. Pharm. Sci. Technol. 62 (2008), pp. 256–263.
[31] S. Amin, K. Kohli, R.K. Khar, S.R. Mir, and K.K. Pillai, *Mechanism of* in vitro *percutaneous absorption enhancement of carvedilol by penetration enhancers*, Pharm. Dev. Technol. 13 (2008), pp. 533–539.
[32] L. Wei, P. Sun, S. Nie, and W. Pan, *Preparation and evaluation of SEDDS and SMEDDS containing carvedilol*, Drug Dev. Ind. Pharm. 31 (2005), pp. 785–794.
[33] W. Warisnoicharoen, A.B. Lansley, and M.J. Lawrence, *Nonionic oil-in water microemulsions: The effect of oil type on phase behaviour*, Int. J. Pharm. 198 (2000), pp. 7–27.
[34] P.K. Ghosh, R.J. Majithiya, M.L. Umrethia, and R.S.R. Murthy, *Design and development of microemulsion drug delivery system of acyclovir for improvement of oral bioavailability*, AAPS PharmSciTech. 7 (2006), pp. E1–E6.
[35] M. Malmstein, *'Microemulsion in pharmaceuticals*, in *Handbook of Microemulsion: Science and Technology*, P. Kumar and K.L. Mittal, eds., Marcel Dekker, New York, 1999, pp. 755–772.
[36] A.A. Date and M.S. Nagarsenker, *Design and evaluation of self-nanoemulsifying drug delivery systems (SNEDDS) for cefpodoxime proxetil*, Int. J. Pharm. 329 (2007), pp. 166–172.
[37] C. Malcolmson, A. Sidhu, C. Satra, S. Kantaria, and M.J. Lawrence, *Effect of the nature of oil on the incorporation of testosterone propionate into non-ionic oil-in-water microemulsions*, J. Pharm. Sci. 87 (1998), pp. 109–116.
[38] M. Fukuda, *The importance of lipophobicity in surfactants: Methods for measuring lipophobicity and its effect on the properties of two types of nonionic surfactant*, J. Colloid Interface Sci. 289 (2005), pp. 512–520.
[39] P. Izquierdo, D.P. Acharya, K. Hirayama, H. Asaoka, K. Ihara, T. Tsunehiro, Y. Shimada, Y. Asano, S. Kokubo, and H. Kunieda, *Phase behaviour of pentaglycerol monostearic and monooleic acid esters in water*, J. Dispersion Sci. Technol. 27 (2006), pp. 99–103.
[40] L. Djekic and M. Primorac, *The influence of cosurfactants and oils on the formation of pharmaceutical microemulsions based on PEG-8 caprylic/capric glycerides*, Int. J. Pharm. 352 (2008), pp. 231–239.
[41] L. Djordjevic, M. Primorac, and M. Stupar, In vitro *release of diclofenac diethylamine from caprylocaproyl macrogolglycerides based microemulsions*, Int. J. Pharm. 296 (2005), pp. 73–79.
[42] A.M. Moreno, M.P. Ballesteros, and P. Frutos, *Lecithin-based oil-in-water microemulsions for parenteraluse: Pseudoternary phase diagrams, characterization and toxicity studies*, J. Pharm. Sci. 92 (2003), pp. 1428–1437.
[43] H. Chen, X. Chang, T. Weng, X. Zhao, Z. Gao, Y. Yang, H. Xu, and X. Yang, *A study of microemulsion systems for transdermal delivery of triptolide*, J. Control. Release 98 (2004), pp. 427–436.
[44] H. Chen, X. Chang, D. Du, J. Li, H. Xu, and X. Yang, *Microemulsion based hydrogel formulation of ibuprofen for topical delivery*, Int. J. Pharm. 315 (2006), pp. 52–58.
[45] A.C. Sintov and L. Shapiro, *New microemulsion vehicle facilitates percutaneous penetration* in vitro *and cutaneous drug bioavailability* in vivo, J. Control. Release 95 (2004), pp. 173–183.
[46] H.O. Ho, C.C. Hsiao, and M.T. Sheu, *Preparation of microemulsions using polyglycerol fatty acid esters as surfactant for the delivery of protein drugs*, J. Pharm. Sci. 85 (1996), pp. 138–143.

[47] Product information sheet, Miglyol® 810, 812, 818, 829, 840. Neutral Oils for Pharmaceuticals and Cosmetics, Sasol Germany GmbH Oleochemicals. Witten, Germany. Available at http://www.sasol.com.
[48] Y.-S. Rhee, J.-G. Choi, E.-S. Park, and S.-C. Chi, *Transdermal delivery of ketoprofen using microemulsions*, Int. J. Pharm. 228 (2001), pp. 161–170.
[49] B. Baroli, M.A. Lopez-Quintela, M.B. Delgado-Charro, A.M. Fadda, and J. Blanco-Mendez, *Microemulsions for topical delivery of 8-methoxsalen*, J. Control Release 69 (2000), pp. 209–218.
[50] G.L. Flynn and B. Stewart, *Percutaneous drug penetration: Choosing candidates for transdermal development*, Drug Dev. Res. 13 (1988), pp. 169–185.